Fiberized Silicon Devices for All-Optical Signal Processing

Fariza H Suhailin[1,*], Noel Healy[2] and Anna C Peacock[3]

[1] School of Fundamental Science, Universiti Malaysia Terengganu, 21300 Kuala Terengganu, Malaysia
[2] Emerging Technology and Materials Group, Newcastle University, Newcastle upon Tyne, NE1 7RU, UK
[3] Optoelectronics Research Centre, University of Southampton, Southampton SO17 1BJ, UK
*farizahanim@umt.edu.my

***Abstract*—Recent fabrication techniques have enabled the incorporation of crystalline and amorphous silicon materials inside silica capillaries to produce optical fibers with the silicon photonics capability. This paper will review the recent efforts to develop compact nonlinear devices from silicon fiber platform. These fiber-based devices will be of great interest for applications in all-optical signal processing.**

Keywords—silicon fiber; nonlinear devices; all-optical signal processing

I. INTRODUCTION

Silicon is a key material for semiconductor photonics and has underpinned much of the recent growth in this field. Technological breakthroughs such as signal amplification, light generation [1], and all-optical modulator [2] have been demonstrated in silicon waveguides. All of these have relied on the exploitation of silicon's high third order nonlinearity, $\chi^{(3)}$ [3]. However, a prominent challenge for the planar devices is to achieve an efficient coupling of light between the conventional fiber network to the waveguide. Recently, a new class of optical fibers with semiconductor core and silica glass cladding has been fabricated using one of two distinct paradigms; modified chemical vapor deposition (CVD) [4] or molten core drawing (MCD) [5]. One major distinction between the two techniques is the temperature regime that they operate at. The lower temperature CVD approach allows step-index fibers with hydrogenated amorphous silicon (a-Si:H) core of ~2 μm and ~6 μm in diameters to be produced, while the high temperature MCD approach produces fibers with large poly-crystalline (p-Si) cores (16-50 μm), but has the advantage of producing long kilometer lengths. These semiconductor fibers maintain many of the advantageous properties of the commercial silica fiber such as robustness and flexibility, as well as offering the potential for seamless integration within existing networks. However, much of the initial attention was given on a-Si:H core fibers due to the large Kerr nonlinear refractive index, n_2, and relatively modest nonlinear two-photon absorption (TPA), β_{TPA}, at telecom wavelengths, which combined provide a high nonlinear figure of merit (FOM) [6-8]. Furthermore, advances have been made with regards using standard optical fiber post processing techniques to tailor the waveguide properties beyond that achievable in the on-chip counterpart.

In this paper, we will review the first steps towards device fabrication via post-processing the silicon core fibers. Novel geometries such as tapered silicon waveguides and whispering gallery mode (WGM) microresonators were fabricated from silicon core fibers. These devices offer a unique approach to tune the light confinement to enhance the nonlinear interactions and achieve a high speed optical signal processing. In the first section of this paper, we will describe the characterization of the silicon core fibers, from which the fibers will be post-processed to realize novel devices. This will be followed with the fabrication details and the experiments to demonstrate device functionalities, for the use of signal modulation and processing.

II. CHARACTERIZATION OF SILICON CORE FIBERS

The nonlinear pulse propagation in silicon core fibers can be described by modified nonlinear Schrödinger equations (NLSE) [8]:

$$\frac{\partial A}{\partial z} = \frac{-i\beta_2}{2}\frac{\partial^2 A}{\partial t^2} + i\gamma|A|^2A - \frac{1}{2}(\sigma_{\mathrm{FCA}} + \alpha_l)A, \qquad (1)$$

$$\frac{\partial N_c}{\partial t} = \frac{\beta_{\mathrm{TPA}}}{2h\nu_0}\frac{|A|^4}{A_{\mathrm{eff}}^2} - \frac{N_c}{\tau_c}, \qquad (2)$$

where A represent the slowly varying pulse envelope, β_2 is the group velocity dispersion (GVD) and α_l is the linear loss. The complex nonlinear parameter is given by: $\gamma = k_o n_2/A_{\mathrm{eff}} + i\beta_{\mathrm{TPA}}/2A_{\mathrm{eff}}$, in terms of the Kerr n_2 and the TPA coefficients β_{TPA}, as well as the fiber mode area A_{eff}. The free-carrier parameter is described by: $\sigma_{\mathrm{FCA}} = \sigma\,(1+ i\mu)\,N_c$, where σ is free-carrier absorption, μ is the free-carrier dispersion and τ_c is the carrier lifetime. Using this form of the NLSE to fit the experimental results, we have determined the nonlinear parameters for the ~6 μm a-Si:H core fiber with α_l = 2.1 dB/cm at 1.54 μm to be: β_{TPA} = 0.70 cm/GW, σ_{FCA}= 1.0×10^{-16} cm^2 and n_2 = 1.71×10^{-13} cm^2/W, to yield a FOM ~1.6, which is around two to three times larger than that of crystalline silicon (c-Si) at this wavelength [8, 9]. More recently, significant efforts to optimize the fabrication process have produced low loss fibers with α_l = 0.9 dB/cm at 1.54 μm and reducing to 0.29 dB/cm as the wavelength is increased out to the mid-infrared regime at 2.7 μm [10, 11]. For the smaller core fibers with diameters ~2 μm, the linear loss of α_l = 2.8 dB/cm at 1.54 μm is only slightly higher than the ~6 μm a-Si:H fibers, and the value drops to 0.8 dB/cm at 2.4 μm wavelength [10]. It is worth highlighting that all of the initial nonlinear characterizations in silicon fibers have been performed on the deposited fibers with a-Si:H core materials. The large core, as-drawn p-Si fibers usually exhibit losses greater than 20 dB/cm, which in particular, will preclude nonlinear pulse transmission in the fibers.

III. TAPERED POLYSILICON FIBER DEVICES

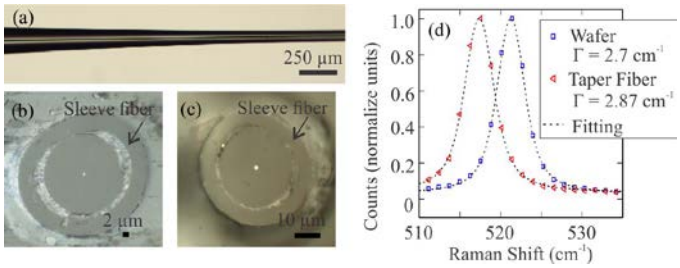

Fig. 1. (a) Longitudinal image of a tapered p-Si fiber. Polished cross sections of (b) 0.6 μm and (c) 0.9 μm core. (d) Raman spectra for the submicron core tapered p-Si. The dashed curves are the Voigt fits, and the Lorentzian linewidths are given in the legend [12, 13].

The p-Si material holds great potential for the development of cheaper and flexible on-chip photonics platforms that can be integrated into multilayer and large scale architectures [14, 15]. The optical and electronics properties of p-Si materials can be comparable to c-Si, making p-Si a promising material for future optoelectronics devices. However, the high optical loss in p-Si, which is due to the light absorption and scattering at the grain boundaries, make producing high performance devices challenging [14]. For the case of p-Si fibers, different post-processing methods have been employed to improve the material quality and yield low loss fibers. For instance, the lowest losses reported for furnace annealed p-Si fibers with ~6 μm core dimensions are in range of 6-8 dB/cm [16]. However, the losses can be further reduced to 5 dB/cm in the 2 μm core fibers and 2 dB/cm in the large 10 μm core fibers when treated with a laser annealing process [17, 18]. An alternative post-processing method makes use of a fiber tapering procedure. Tapering will introduced longitudinal variations to the size of the fiber to reduce the core dimension for higher light confinement. The heating and melting during the tapering will recrystallize the core can increase the grain size [19], which is vital to reduce the transmission loss in the p-Si fibers. Significantly, with a combination of the small (few microns to hundreds of nanometer-sized) core dimension and low transmission loss, a framework to develop nonlinear fibers from the p-Si can be realized.

Our work has pursued a modified tapering method to post-process the ~10 μm core p-Si fibers [12]. The fiber is first sleeved inside a thick silica capillary and then tapered using a hot filament. During the procedure, both the silica sleeve and fiber cladding will soften, while the molten core will take the shape of the cladding and recrystallized as it cools. Fig. 1(a) shows the longitudinal image of a tapered p-Si fiber with a smooth and continuous transition along the length. We obtained a range of core sizes and Fig. 1(b,c) shows the cross-sections of 0.6 μm and 0.9 μm tapered fibers, respectively. The Raman spectra, as shown in Fig. 1(d), indicates an enhanced crystallization in the p-Si core due to the tapering process, where the wavenumber is reduced closer to that of the c-Si reference. Notably, the downshift in the position of the Raman peak with respect to the reference is due to stress induced in the core material [4].

The transmission measurements within the submicron core tapered fiber resulted in the lowest recorded value of α_l = 3.5 dB/cm for any p-Si waveguide. This has subsequently allowed for the first demonstration of nonlinear pulse propagation in this material, as shown in Fig. 2. Fitting these results with the NLSE reveals the best values of β_{TPA} = 0.7 cm/GW, σ_{FCA}= 1.45×10^{-17} cm^2, and n_2 = 5×10^{-14} cm^2/W. Notably, these parameters are within the range of high quality c-Si waveguides [20], verifying the benefit of post-tapering processes for improving the material quality and the overall performance of the fibers. Furthermore, our work has set the foundation to grow single c-Si within the core of optical fibers [13], which would be interesting for the development of in-fiber electronics devices.

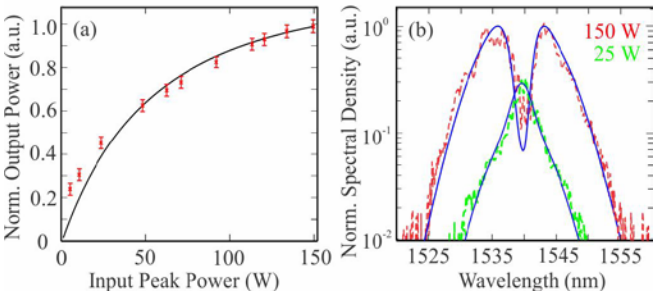

Fig. 2. Nonlinear transmission measurements in 0.9 μm core tapered p-Si fiber. (a) Nonlinear absorption as a function of coupled input power. (b) Spectra evolution at 25 W and 150 W coupled peak powers. Solid curves are for numerical simulation fitting [12].

IV. SILICON-BASED WHISPERING GALLERY MODE MICRORESONATORS

Power efficient, compact and ultrafast data processing schemes are required to facilitate high bandwidth communication networks. However, recent demonstrations of signal modulation and processing in silicon waveguides have all required high powers [7, 21]. Optical micro-resonators with high quality factors (Q) can strongly confine light both spatially and temporally to provide high intracavity intensity for reduced nonlinear thresholds. Thus, the microresonator is ideally suited to performing signal modulation at low powers. In our experiments, the mechanism for signal processing in a microresonator is based on the nonlinear refractive index change, which is instantaneous and acts to shift the position of the WGM resonance. If a week probe is centered on the resonance of the 'cold' cavity, the index change will switch the weak probe into and out of the resonance mode, as such the probe will be turned on-and-off. The three main mechanisms for signal modulation in microresonator are Kerr nonlinearity, thermo-optic effect and free-carrier refraction [22-24], but the former is a more preferable approach as the Kerr nonlinearity has a response time on the order of femtoseconds (fs) for ultrafast signal manipulation.

Fig. 3 shows the silicon fibers that have been post-processed to form microresonators. The cylindrical microresonator (Fig. 3(a)) is fabricated by etching away the silica cladding from the ~6 μm core a-Si:H fiber, and the spherical microresonator (Fig. 3(b)) is fabricated by heating the tip of p-Si fiber (dimension as shown in Fig. 3(c)) with a series of stable CO_2 laser pulses to form a hybrid silica glass/p-Si core microresonator with 115 μm outer and 108 μm inner diameters, respectively. The characterization from the transmission spectrum of both resonators results in a loaded Q_l ~2×10^4 and Q_l ~2×10^5 in the cylindrical and spherical micro-resonators, respectively. Notably, the improvement of Q_l in the spherical microresonator is due to the hybrid configuration, where the WGMs are largely confine within the low loss cladding and the spherical

shaping provides higher mode confinement. The high Q_l and Kerr nonlinearity

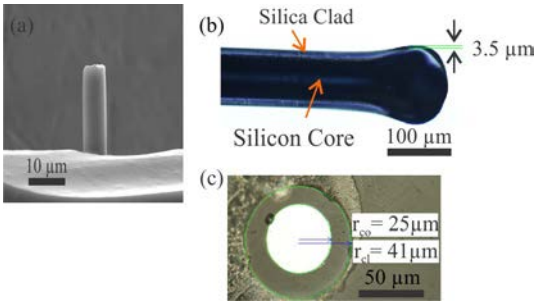

Fig. 3. (a) SEM image of the a-Si:H cylindrical microresonator [25]. (b) Microscope image of the hybrid spherical microresonator [26]. (c) A cross-sectional image of the starting p-Si fiber.

have resulted large Kerr shifts in the WGM resonances under fs pump excitation and these have afforded an opportunity for the first demonstration of ultrafast signal processing in silicon fiber-based microresonators.

The CW signal modulation via pump-probe measurements in a-Si:H cylindrical and hybrid spherical microresonators are shown in Fig. 4. The ~3 dB modulated signal in Fig. 4(a) is achieved when fs pulses with P_{ave} ~20 μW (P_p ~20 mW) are coupled into the a-Si:H cylindrical microresonator via an on-resonance pumping configuration. However, the recorded switching threshold is as low as P_{th} ~5 μW (P_p ~5 mW), which corresponds to only 0.3 pJ pump energy. The switching time is on the order of cavity lifetime, τ ~10 ps. For the hybrid silica glass/p-Si core spherical microresonator, the ~6 dB modulated probe in Fig. 4(b) is recorded at pump P_{ave} ~10 mW. Due to the off-resonance pumping configuration, i.e., the pump is not coupled into the resonator, it is not possible to determine the switching threshold for this cavity. However, in this instance, we expect the on/off switching time to be on the order of sub-picosecond pump, which is an order of magnitude faster than our a-Si:H cylindrical microresonator.

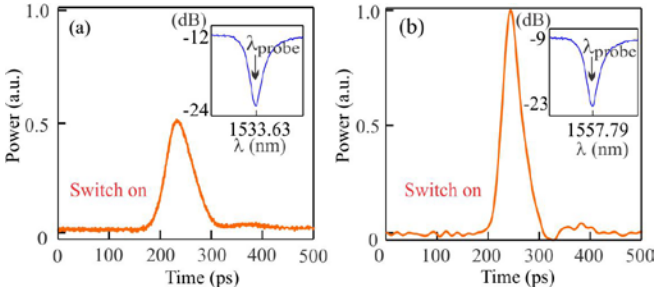

Figure 4. All-optical Kerr switching of weak CW probe in (a) a-Si:H cylindrical microresonator [28] and (b) hybrid spherical microresonator [16]. Insets: the position of CW probe with respect to cold cavity resonance dip.

V. Conclusion

The silicon core fibers have been post-processed to fabricate highly functional nonlinear devices for ultrafast all-optical signal processing. These novel geometries possess favourable properties for a compact and all-fiberized optoelectronics. We strongly believe that silicon core fibers could be utilized in much wider ranging applications including sensor development and fundamental science investigations.

References

1. Liang, D. and J.E. Bowers, *Recent Progress in Lasers on Silicon.* Nature Photonics, 2010. **4**(8): p. 511-517.
2. Reed, G.T., et al., *Silicon Optical Modulators.* Nature Photonics, 2010. **4**(8): p. 518-526.
3. Leuthold, J., C. Koos, and W. Freude, *Nonlinear Silicon Photonics.* Nature Photonics, 2010. **4**(8): p. 535-544.
4. Sazio, P.J.A., et al., *Microstructured Optical Fibers as High-Pressure Microfluidic Reactors.* Science, 2006. **311**(5767): p. 1583-1586.
5. Ballato, J., et al., *Silicon Optical Fiber.* Optics Express, 2008. **16**(23): p. 18675-18683.
6. Mehta, P., et al., *Ultrafast Wavelength Conversion via Cross-Phase Modulation in Hydrogenated Amorphous Silicon Optical Fibers.* Optics Express, 2012. **20**(24): p. 26110-26116.
7. Mehta, P., et al., *All-Optical Modulation Using Two-Photon Absorption in Silicon Core Optical Fibers.* Optics Express, 2011. **19**(20): p. 19078-19083.
8. Mehta, P., et al., *Nonlinear Transmission Properties of Hydrogenated Amorphous Silicon Core Optical Fibers.* Optics Express, 2010. **18**(16): p. 16826-16831.
9. Narayanan, K. and S.F. Preble, *Optical Nonlinearities in Hydrogenated-Amorphous Silicon Waveguides.* Optics Express, 2010. **18**(9): p. 8998-9005.
10. Shen, L., et al., *Nonlinear Transmission Properties of Hydrogenated Amorphous Silicon Core Fibers Towards the Mid-Infrared Regime.* Optics Express, 2013. **21**(11): p. 13075-13083.
11. Mehta, P., et al., *Effect of Core Size on Nonlinear Transmission in Silicon Optical Fibres*, in *Lasers and Electro-Optics Conference (CLEO)*. 2012: San Jose.
12. Suhailin, F.H., et al., *Tapered Polysilicon Core Fibers for Nonlinear Photonics.* Optics Letters, 2016. **41**(7): p. 1360-1363.
13. Franz, Y., et al., *Material Properties of Tapered Crystalline Silicon Core Fibers.* Optical Materials Express, 2017. **7**(6): p. 2055-2061.
14. Kwong, D., et al., *Ultralow-Loss Polycrystalline Silicon Waveguides and High Uniformity 1x12 MMI Fanout for 3D Photonic Integration.* Optics Express, 2012. **20**(19): p. 21722-21728.
15. Preston, K. and M. Lipson, *Slot Waveguides with Polycrystalline Silicon for Electrical Injection.* Optics Express, 2009. **17**(3): p. 1527-1534.
16. Lagonigro, L., et al., *Low Loss Silicon Fibers for Photonics Applications.* Applied Physics Letters, 2010. **96**(4): p. 0411051-0411053.
17. Healy, N., et al., *Extreme Electronic Bandgap Modification in Laser-Crystallized Silicon Optical Fibres.* Nature Materials, 2014. **13**(12): p. 1122-1127.
18. Healy, N., et al., *CO2 Laser-Induced Directional Recrystallization to Produce Single Crystal Silicon-Core Optical Fibers with Low Loss.* Advanced Optical Materials, 2016: p. 1-5.
19. McMillen, C., et al., *On Crystallographic Orientation in Crystal Core Optical Fibers II: Effects of Tapering.* Optical Materials, 2012. **35**(2): p. 93-96.
20. Yin, L. and G.P. Agrawal, *Impact of Two-Photon Absorption on Self-Phase Modulation in Silicon Waveguides.* Optics Letters, 2007. **32**(14): p. 2031-2033.
21. Mathlouthi, W., H. Rong, and M. Paniccia, *Characterization of Efficient Wavelength Conversion by Four-Wave Mixing in Sub-Micron Silicon Waveguides.* Optics Express, 2008. **16**(21): p. 16735-16745.
22. Pöllinger, M. and A. Rauschenbeutel, *All-Optical Signal Processing at Ultra-Low Powers in Bottle Microresonators using the Kerr Effect.* Optics Express, 2010. **18**(17): p. 17764-17775.
23. Almeida, V.R. and M. Lipson, *Optical Bistability on a Silicon Chip.* Optics Letters, 2004. **29**(20): p. 2387-2389.
24. Xu, Q. and M. Lipson, *Carrier-Induced Optical Bistability in Silicon Ring Resonators.* Optics Letters, 2006. **31**(3): p. 341-343.
25. Vukovic, N., et al., *Ultrafast Optical Control using the Kerr Nonlinearity in Hydrogenated Amorphous Silicon Microcylindrical Resonators.* Scientific Reports, 2013. **3**: p. 2885.

26. Suhailin, F.H., et al., *Kerr nonlinear switching in a hybrid silica-silicon microspherical resonator*. Optics Express, 2015. **23**(13): p. 17263-17268.

The authors acknowledge EPSRC (EP/G051755/1, EP/J004863/1, and EP/I035307/1), NSF (DMR-1107894), NORFAB, Norwegian Discovery Fund and Penn State Materials Research Science and Engineering Center (NSF DMR-0820404) for financial support.